Functional Specialisation and Effective Connectivity During Self-paced Unimanual and Bimanual Tapping of Hand Fingers: An Extended Analysis Using Dynamic Causal Modeling and Bayesian Model Selection for Group Studies

[1]Ahmad Nazlim Yusoff *, [1]Aini Ismafairus Abd Hamid, [1]Khairiah Abdul Hamid, [2]Wan Ahmad Kamil Wan Abdullah, [1]Mazlyfarina Mohamad & [1,3]Hanani Abdul Manan

[1]Functional Image Processing Laboratory (FIPL), Diagnostic Imaging & Radiotherapy Program, Faculty of Health Sciences, Universiti Kebangsaan Malaysia, Jalan Raja Muda Abdul Aziz, 50300 Kuala Lumpur, Malaysia

[2]Department of Radiology, School of Medical Sciences, Universiti Sains Malaysia, 16150 Kubang Kerian, Kelantan

[3]Medical Imaging Department, Faculty of Therapeutic Sciences, Masterskill University College of Health Sciences, G-8, Jalan Kemacahaya, Batu 9, 43000 Cheras, Selangor

ABSTRACT

Introduction: This multiple-subject fMRI study continue to further investigate brain activation within and effective connectivity between the significantly (p<0.001) activated primary motor area (M1), supplementary motor area (SMA) with the inclusion of BA44 during unimanual (UNI_{right} and UNI_{left}) and bimanual (BIM) self-paced tapping of hand fingers. **Methods:** The activation extent (spatial and height) and effective connectivity were analysed using statistical parametric mapping (SPM), dynamic causal modeling (DCM) and the novel method of Bayesian model selection (BMS) for group studies. **Results:** Group results for UNI_{right} and UNI_{left} showed contra-lateral and ipsi-lateral involvement of M1 and SMA. The results for BIM showed bilateral activation in M1, SMA and BA44. A larger activation area but with lower percentage of signal change (PSC) are observed in the left M1 due to the control on UNI_{right} as compared to the right M1 due to the control on UNI_{left}. This is discussed as due to the influence of the tapping rate effects that is greater than what would be produced by the average effects of the dominant and sub-dominant hand. However, the higher PSC observed in the right M1 is due to a higher control demand used by the brain in coordinating the tapping of the sub-dominant hand fingers. Connectivity analysis indicated M1 as the intrinsic input for UNI_{right} and UNI_{left} while for BIM, the inputs were both M1s. During unilateral finger tapping, the contra-lateral M1 acts as the input center which in turn triggers the propagation of signal unidirectionally to other regions of interest. The results obtained for BIM (BIM_{left} and BIM_{right}) however yield a model with less number of significant connection. M1-M1 connection is unidirectional for UNI_{left} and UNI_{right} originating from contra-lateral M1, and is inhibited during BIM. **Conclusion:** By taking into consideration the presence of outliers that could have arisen in any subject under study, BMS for group study has successfully chosen a model that has the best balance between accuracy (fit) and complexity.

Keywords: **Primary motor area, Supplementary motor area, BA44, Bayes rule, Statistical Parametric Mapping**

INTRODUCTION

In spite of a vast number of research conducted in studying how uni- and bimanual motor action are coordinated by the brain[1–3], questions still arise about the exact mechanism underlying the existence of activation clusters in the contra-lateral as well as in the ipsi-lateral regions and their functional relationships. These pertaining, in particular, to the height and spatial extent of activation in the respective motor associated areas as well as the strength and direction of the connections between those areas. With the inception of several novel computational neuroscience approaches in studying connectivity i.e. structural equation modeling (SEM)[4] and dynamic causal modeling (DCM)[5], the number of works conducted in studying brain dynamic escalated dramatically, focusing not only among the areas in one region but also with the areas in the other brain regions[1-3].

A comprehensive assessment of uni- and bimanual hand movements covering the aspects of functional specialisation and effective connectivity has been reported[1]. They studied the dynamic intra- and interhemispheric interactions among the motor regions by means of functional magnetic resonance imaging (fMRI) and dynamic causal modeling (DCM). They found that the uni- and bimanual types of hand movement did modulate the neural coupling within the motor

*Corresponding author: *nazlim@fskb.ukm.my*

network. The excitation and inhibition of neural activity found in their study were evidences of dynamic interplay of various motor regions, in particular the primary motor cortex (M1), supplementary motor area (SMA) and pre motor cortex (PMC). They also suggested that the SMA represents the key structure in promoting or suppressing the activity in the cortical motor network during both types of movement. With the aid of DCM, they had successfully modeled the intrinsic connectivity among motor regions modulated by sensory input that are generated via visual instructions. Their works however concentrated only on the connectivity between motor related regions which were activated at corrected alpha value. The use of a high threshold will certainly exclude regions of mild activation regardless of the existence of their connection with the primary motor regions. As a result, significant connections between areas of mild responses with those significantly high may be unintentionally left unattended.

Another novel work on motor activation and network in human[3] reported that the dominant hemisphere is responsible in initiating the control over bilateral movement. They also discovered that bilateral activation is not the sum of the right and left unilateral activation from which it was later indicated that the left and right unimanual movements differ significantly in terms of the activation of and connectivities between the areas involved. They finally concluded that by using SEM, as opposed to other study[1] that made use of DCM, individual subject and group network identification has been made possible.

SEM however, rests on the assumptions that the interaction between independent variables is linear and the data are instantaneous and conservative. Since the observed blood oxygenation level dependent (BOLD) signal is time-series which rendered the data non conservative and that there is always a possibility that the interaction between any two regions is non linear, BOLD signal can only be explained by combining both the expressions for the neuronal and hemodynamic levels[6] as encapsulated in DCM. Therefore, DCM is the preferred approach for fMRI data. Implementing DCM will result in a complete model for fMRI, from which it is understood that the effective connectivity expressed at the level of neurodynamics, will cause changes in the observed hemodynamics or BOLD signal. A detailed explanation on the comparison between SEM and DCM in modeling functional integration has been given elsewhere[7].

It has been established that the primary motor area (M1) in the precentral gyrus (PCG), the supplementary motor area (SMA) and premotor cortex (PMC) are involved in movement preparation and execution of motor action[8]. However, motor coordination is not limited only to those three areas especially when modulatory inputs come into play. For example, areas that are involved in processing sound, speech and language such as BA41, BA44 and BA45 may also be activated during a motor activation task if the instruction is verbally or auditorily given. Having that in mind, establishing a reliable model of how these areas interact is crucial for a wider understanding of the mechanism underlying motor function. This was also found to be useful for both healthy subjects and patients[1]. The modeled interaction will certainly find its importance since the present knowledge on functional specialisation and organization of human brain is limited and still lacking[9].

Many previous finger tapping studies[1, 10 & 11] relied on systematically contained instructions visually or auditorily given to the subjects. The externally triggered stimuli will then evoke responses not only in motor areas but also in areas related to vision, hearing and cognition. This will certainly complicate the study of connectivity between motor areas but will enhance the networks further outside motor regions. More information will be gained since motor areas could also be connected to other associated areas in the cortex. In this study, the subjects were instructed to perform self-paced tapping of right, left or bimanual hand fingers, at moderate tapping force and speed, cued by auditory instruction given in a very short duration.

This study is a continuation of our previous work on single[12] and multiple subjects[12-15]. In this study, the brain functional specialisation and integration were investigated on multiple subjects with regards to the activation in the cerebral motor cortices evoked by unimanual and bimanual finger tapping which were robustly done by the subjects. First, group analyses were conducted by means of random effects analysis (RFX) and inferences based on the group responses were made onto the whole subject at a relatively low significant level ($\alpha = 0.001$) uncorrected for multiple comparisons. The motivation is to search for motor areas and other areas not related to motor areas but are also activated with significant connectivity with the motor areas. Brain activation at low significant level has also been previously reported[16-18]. A low alpha threshold is thought to be suitable for group studies that consist of a relatively high between-subjects variability.

Secondly, the connectivity measure between regions of interest (ROIs) were studied and evaluated by implementing the dynamic causal modeling (DCM) to model interactions among neuronal populations at cortical level. Prior to input determination, full connectivity models with various inputs are initially constructed for UNI_{right}, UNI_{left} and BIM based on the ROIs defined in the RFX and estimated using DCM. The estimated models are then compared in a Bayesian framework. Finally, the most probable model with predetermined input was then reduced to a model with significant connections that would represent the intrinsic couplings during unimanual and bimanual tapping of hand fingers for all subjects.

As opposed to our previous study[13] that uses Akaike Information Criterion (AIC) and Bayesian Information Criterion (BIC)[9] in selecting the most optimum model, this study uses a novel BMS approach for group study in

searching for a model that has the best balance between accuracy (fit) and complexity and a model that best represent the observed BOLD signal. More importantly, the results obtained from group BMS studies, while being able to reproduce results of group Bayes factor (GBF) and positive evidence ratio (PER) as explained in our previous study[15], are reported[19] to be able to take into consideration the presence of outliers that could have arisen in any subject under study. While GBF is very sensitive to outliers (magnitude of differences across subjects) and PER can only describe the qualitative reproducibility of model comparison over subjects, BMS analysis for group study is the preferred approach in model comparison involving multiple subjects.

METHODS

Subject

Functional magnetic resonance imaging (fMRI) examinations were performed on 16 right-handed subjects (4 males and 12 females). The subjects were given informed consent and screening forms as required by the Institutional Ethics Committee (IEC). The subjects were interviewed on their health condition prior to the scanning session. Prior to the fMRI scans, the subjects' handedness was tested using the Edinburgh Handedness Inventory[20]. The subjects were also told not to move their head during the scan to avoid serial correlation and drift. Head movement will also cause artifacts on functional images due to the voxels that are not correctly registered (or moving) during the scan resulting in significant changes in signal intensity of that particular voxels over time[21]. The immobilising devices were used together with the head coil in order to minimise head movement.

fMRI Scans

Functional magnetic resonance imaging (fMRI) examinations were conducted using a 1.5-tesla magnetic resonance imaging (MRI) system (Siemens Magnetom Vision VB33G) equiped with functional imaging option, echo planar imaging (EPI) capabilities and a radiofrequency (RF) head coil used for signal transmission and reception. Gradient Echo - Echo Planar Imaging (GRE-EPI) pulse sequence with the following parameters were applied : repetition time (TR) = 5 s, acquisition time (TA) = 3 s, echo time (TE) = 66 ms, field of view (FOV) = 210 × 210 mm, flip angle = 90^{o}, matrix size = 128 × 128 and slice thickness = 4 mm. Using the midsagittal scout image (TR = 15 ms, TE = 6 ms, FOV = 300 × 300 mm, flip angle = 30^{o}, matrix size = 128 × 128 and magnetic field gradient = 15 mT/m) produced earlier, 35 axial slice positions (1 mm interslice gap) were oriented in the anterior-posterior commissure (AC-PC) plane. This covers the whole brain volume. In addition, high resolution anatomical images of the entire brain were obtained using a strongly T1-weighted spin echo pulse sequence with the following parameters : TR = 1000 ms, TE = 30 ms, FOV = 210 × 210 mm, flip angle = 90^{o}, matrix size = 128 × 128 and slice thickness = 4 mm[12].

Experimental paradigm

The subjects were instructed on how to perform the motor activation task and were allowed to practice prior to the scanning. The subjects had to tap all four fingers against the thumb beginning with the thumb-index finger contact and proceeding to the other fingers in sequence which would then begin anew with contact between thumb and index finger. This study used a robust self-paced finger movement. The tapping of the fingers would approximately be two times in one second (using an intermediate force between too soft and too hard). A six-cycle active-rest paradigm which was alternately and auditorily cued between active and rest was used with each cycle consisting of 10 series of measurements during active state and 10 series of mesurements during resting state. The tapping of the fingers were done unimanually (UNI_{left} or UNI_{right}) or bimanually (BIM) in an alternate fashion[12]. Each functional measurement produces 20 axial slices in 3 s (one image slice in 150 ms) with an inter-measurement interval of 2 s. The measurement starts with active state. The imaging time for the whole functional scan was 600 s (10 minutes) which produced 120 × 20 = 2400 images in total. High resolution T2*-weighted images were obtained using the voxel size of 1.64 mm × 1.64 mm × 4.00 mm.

Post processing of the fMRI data

All the functional (T2*-weighted) and structural (T1-weighted) images were analysed using a personal computer (PC) with a high processing speed and large data storage. The MATLAB 7.4 – R2007a (Mathworks Inc., Natick, MA, USA) and Statistical Parametric Mapping (SPM5 and SPM8) (Functional Imaging Laboratory, Wellcome Department of Imaging Neuroscience, Institute of Neurology, University College of London) software packages were used for that purpose. The raw data in DICOM (.dcm) format were transformed into Analyze (.hdr, .img) format and preprocessed by means of SPM5. Functional images in each measurement were realigned using the 6-parameter affine transformation in translational (*x, y* and *z*) and rotational (pitch, roll and yaw) directions to reduce artifacts from subject movement and in order to make within and between subject comparison a meaningful way. After realigning the data, a mean

image of the series is used to estimate some warping parameters that map it onto a template that already conforms to a standard anatomical space (EPI template provided by the Montreal Neurological Institute - MNI). The normalisation procedure used a 12-parameter affine transformation[22]. The images were then smoothed using an 8-mm full-width-at-half-maximum (FWHM) Gaussian kernel. Activated voxels were identified by the general linear model approach by estimating the parameters of the model and by deriving the appropriate test statistic (*T* statistic) at every voxel. Statistical inferences were finally obtained on the basis of random effects analysis (RFX) and the Gaussian random field theory. The inferences were made using the *T*-statistic at significant level (α) = 0.001, uncorrected for multiple comparisons. A detail description on spatial pre processing can be found elsewhere[21].

Region of interest (ROI) Analyses

The cortical brain regions which are found to be significantly activated during the finger tapping task are defined using the Anatomy toolbox[23] at $\alpha < 0.001$, uncorrected for multiple comparisons. The selected regions of interest (ROIs) in this study are the primary motor area (M1), supplementary motor area (SMA) and the opercular part of inferior frontal gyrus or BA44. The peak coordinates of the respective ROI on the statistical parametric maps (SPMs) produced from RFX were taken as the anatomical landmark and the corresponding coordinates for the individual subject. The anatomical constraints for the RFX coordinates as suggested in a previous study[1] are; 1) the M1 coordinates had to be located in the precentral gyrus/sulcus, 2) the SMA coordinates had to be in the dorsal medial wall within the inter-hemispheric fissure. For the coordinates of BA44, they had to be in the area bounded caudally and dorsally by the agranular frontal area 6, dorsally by the granular frontal area 9 and rostrally by the triangular area 45. A spherical volume of 4-mm radius with the ROIs' peak coordinates (Table 1) as the center are defined and named as the left M1 (M1-L), left SMA (SMA-L), left BA44 (BA44-L), right M1 (M1-R), right SMA (SMA-R) and right BA44 (BA44-R). Group's percentage of signal change (PSC) relative to the baseline for all ROIs was extracted from the 4-mm radius sphere using MarsBar toolbox for SPM[24].

Dynamic causal modeling (DCM)

Dynamic causal modeling (DCM) was implemented in evaluating the effective connectivity between the ROIs within and between the right and left hemispheres. A detail explanation of the underlying mathematical and biophysical concepts can be found elsewhere[5] but the basic principle is presented here. DCM is a study of the dynamic of interaction among neuronal populations at cortical level. This is done by modeling the interaction as a dynamic input-state-output system. DCM can be described by the following multivariate bilinear differential equation.

$$\dot{z}_t = \left(\boldsymbol{A} + \sum_{j=1}^{M} u_t(j)\boldsymbol{B}^j\right) z_t + \boldsymbol{C}u_t \qquad (1)$$

In Equation (1), $\boldsymbol{A}$ is the matrix that represents the fixed or context-independent strength of connections between the modeled regions (intrinsic couplings) and the matrices $\boldsymbol{B}^j$ represent the modulation of these connections. The matrix $\boldsymbol{C}$ is free of z_t but its role is to model the extrinsic influences of inputs on neuronal activity. In the absence of u_t, $\dot{z}_t = \boldsymbol{A}z_t$, which implies that the only existing connectivities are that of the intrinsic couplings between the regions of interest (ROIs)[5, 9, 25].

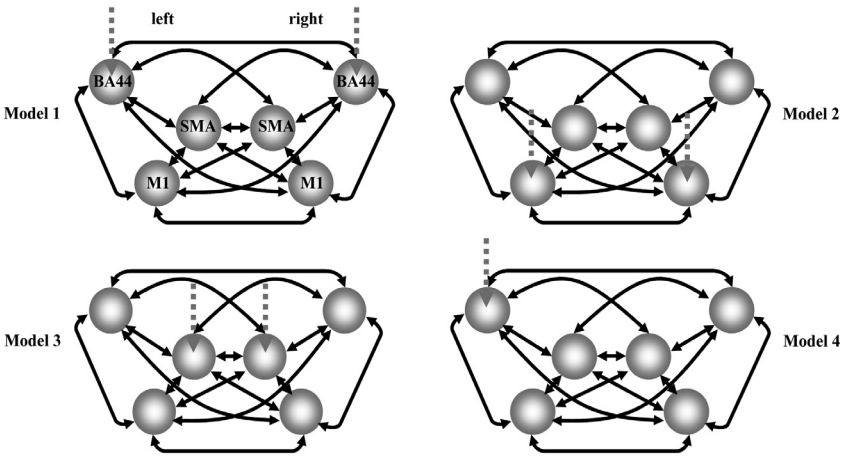

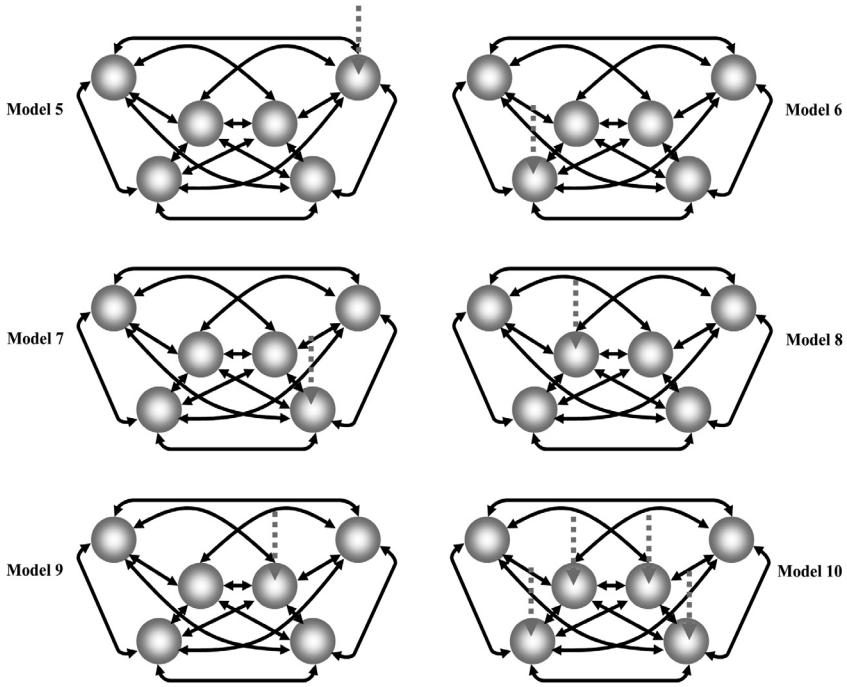

Figure 1: Full connectivity model used in dynamic causal modeling (DCM) in determining the input center for UNI_{right}, UNI_{left} and BIM. The labels for the ROIs are only shown in Model 1. The red dotted arrows represent the input(s) while ↔ represents bidirectional connection

Table 1 a): RFX coordinates for the left and right M1, SMA and BA44 that are obtained from UNI_{right}, UNI_{left} and BIM,

	RFX Coordinates					
	M1-L	M1-R	SMA-L	SMA-R	BA44-L	BA44-R
UNI_{right}	-32 -22 50	-	-6 6 48	-	-54,2,32	-
UNI_{left}	-	38 -20 62	-	6 2 54	-	56,8,32
BIM	-32,-22,50	34,-20,50	-6,6,48	8,8,46	-56,6,22	64,8,22

Table 1 b): The actual coordinates used in the construction of DCMs

		RFX Coordinates					
		M1-L	M1-R	SMA-L	SMA-R	BA44-L	BA44-R
Subject 1	UNI_{right}	-32,-22,50	46,-26,60	-6,6,48	6,2,54	-56,6,30	56,8,32
	UNI_{left}	-32,-22,52	38,-20,62	-6,6,48	6,2,54	-54,2,32	56,8,32
	BIM	-32,-22,50	34,-20,50	-6,6,48	10,8,44	-56,6,22	64,8,22
Subject 2	UNI_{right}	-32,-22,50	36,-18,64	-6,6,48	6,2,54	-54,2,32	56,8,32
	UNI_{left}	-32,-22,50	38,-20,62	-6,6,48	6,2,56	-54,2,32	56,8,32
	BIM	-32,-22,50	34,-20,50	-6,6,48	8,8,46	-56,6,20	64,8,22
Subject 3	UNI_{right}	-32,-22,50	38,-20,60	-6,6,48	8,2,54	-54,2,32	56,8,32
	UNI_{left}	-40,-24,58	38,-20,62	-6,6,48	6,2,54	-54,4,34	56,12,34
	BIM	-32,-22,50	32,-20,50	-4,4,48	8,8,44	-56,8,20	62,10,24

Continuation

Table 1 b): The actual coordinates used in the construction of DCMs

		RFX Coordinates					
		M1-L	M1-R	SMA-L	SMA-R	BA44-L	BA44-R
Subject 4	UNI_{right}	-32,-22,50	38,-20,62	-6,6,48	6,2,54	-54,2,32	56,8,32
	UNI_{left}	-32,-22,50	38,-20,62	-6,6,48	6,2,54	-54,2,32	56,8,32
	BIM	-32,-22,50	34,-20,50	0,6,52	4,8,50	-56,8,22	62,10,20
Subject 5	UNI_{right}	-32,-22,50	38,-20,62	-6,6,48	6,2,54	-54,2,32	6,2,54
	UNI_{left}	-32,-22,50	38,-20,62	-6,6,48	6,2,54	-54,2,32	56,8,32
	BIM	-32,-22,50	34,-20,50	-6,6,48	8,6,46	-56,6,24	64,14,24
Subject 6	UNI_{right}	-32,-22,50	40,-24,60	-6,6,48	8,2,54	-56,4,30	52,6,30
	UNI_{left}	-30,-18,50	38,-20,62	-6,6,48	6,2,52	-54,2,32	56,8,32
	BIM	-32,-22,50	34,-20,50	-6,6,48	8,8,46	-52,2,28	64,8,20
Subject 7	UNI_{right}	-32,-22,50	38,-20,62	-6,6,48	6,2,54	-54,2,32	56,8,32
	UNI_{left}	-36,-22,50	38,-20,62	-6,6,48	6,2,54	-54,2,32	56,8,32
	BIM	-32,-22,50	34,-20,50	-6,6,48	10,8,44	-56,6,22	62,8,14
Subject 8	UNI_{right}	-32,-22,50	34,-18,66	-6,6,48	6,2,54	-54,2,32	56,8,32
	UNI_{left}	-32,-24,50	38,-20,62	-6,6,48	6,2,54	-54,2,32	56,8,32
	BIM	-32,-22,50	34,-20,50	-6,6,48	8,8,46	-56,6,22	64,8,22
Subject 9	UNI_{right}	-32,-22,50	48,-20,62	-6,6,48	6,2,54	-54,4,32	56,10,26
	UNI_{left}	-32,-22,50	38,-20,62	-6,6,48	6,2,54	-54,2,32	56,8,32
	BIM	-32,-22,50	34,-20,50	-6,6,48	12,6,48	-54,6,22	68,0,18
Subject 10	UNI_{right}	-32,-22,50	34,-16,62	-6,6,48	6,2,54	-54,2,32	56,8,32
	UNI_{left}	-32,-22,50	38,-20,62	-6,6,48	6,2,54	-54,2,32	56,8,32
	BIM	-32,-22,50	34,-20,50	-6,6,48	8,8,46	-56,6,22	64,8,22
Subject 11	UNI_{right}	-32,-22,50	34,-10,68	-6,2,48	0,-8,52	-56,6,32	58,8,32
	UNI_{left}	-32,-22,50	38,-20,62	-6,6,48	6,2,54	-54,2,32	56,8,32
	BIM	-32,-22,50	34,-20,50	-6,6,48	8,8,46	-56,6,22	64,8,22
Subject 12	UNI_{right}	-32,-22,50	38,-20,62	-6,6,48	6,2,54	-54,2,32	56,8,32
	UNI_{left}	-32,-22,50	38,-20,62	-6,6,48	6,2,54	-54,2,32	56,8,32
	BIM	-32,-22,50	34,-20,50	-6,6,48	8,8,46	-56,6,22	64,8,22
Subject 13	UNI_{right}	-32,-22,50	36,-14,62	-6,4,48	8,2,52	-54,2,32	56,8,32
	UNI_{left}	-32,-22,50	38,-20,62	-6,6,48	6,2,54	-54,2,32	56,8,32
	BIM	-32,-22,50	34,-20,50	-6,6,48	10,8,46	-56,6,20	62,6,22
Subject 14	UNI_{right}	-32,-22,50	38,-20,62	-6,6,46	6,2,54	-54,2,32	58,8,30
	UNI_{left}	-32,-22,50	38,-20,62	-6,6,48	6,2,54	-54,2,32	56,8,32
	BIM	-32,-22,50	34,-20,50	-6,6,46	8,8,44	-58,8,24	62,8,24
Subject 15	UNI_{right}	-32,-22,50	38,-20,62	-6,6,48	8,0,54	-54,2,32	56,8,32
	UNI_{left}	-30,-22,52	38,-20,62	-6,6,48	6,2,54	-54,2,32	56,8,30
	BIM	-32,-22,50	34,-20,50	-6,6,48	8,6,46	-56,6,22	64,8,22
Subject 16	UNI_{right}	-32,22,50	38,-16,60	-6,6,48	6,2,54	-54,2,32	56,8,32
	UNI_{left}	-36,-26,58	38,-20,62	-4,8,50	6,2,54	-52,2,34	54,10,34
	BIM	-32,-22,50	34,-20,50	-6,6,48	8,8,46	-56,6,22	64,8,22

Full connectivity models with their respective input assumed to be through unilateral and bilateral M1, SMA and/or BA44, were constructed using the above mentioned ROIs (Figure 1). Model construction for BIM used the ROIs' coordinates obtained from RFX. For UNI_{left} and UNI_{right}, the coordinates obtained via RFX are combined together during model construction. The coordinates are shown in Table 1(a). These coordinates were used for all subjects during the construction of VOIs to test for the existence of the effects at uncorrected $\alpha = 0.1$. The final coordinates for model construction are shown in Table 1(b). The models were tested onto all subjects for all UNI_{left}, UNI_{right} and BIM conditions. The estimation procedure was carried out using DCM on the assumption that the interactions between all ROIs are linear. Prior to estimation, the models are specified by including slice timing in the DCMs[6]. The TR for this

study is 5 s which means that the EPI pulse sequence acquires slices at different time over the 5-s duration. Since DCM was not informed about this relatively long TR, it assumed that all slices are acquired simultaneously. As a result, one may obtain unacceptable DCM values if this long time interval is neglected and slice timing is not included in the DCMs. Furthermore, the location of the chosen ROIs in this study is quite distant from each other if measured in the direction perpendicular to slice orientation, rendering the slice timing important in DCM.

The models shown in Figure 1, which have been estimated for UNI_{left}, UNI_{right} and BIM for all subjects were compared using Bayesian model selection (BMS) for group studies. Model comparisons were separately done for UNI_{left}, UNI_{right} and BIM to determine the most probable input centers for the full connectivity models.

The intrinsic connectivity values of the most probable full connectivity models that have been determined for each UNI_{left}, UNI_{right} and BIM were analysed to identify the most probable connection. This is done by first, justifying the connectivity values and their posterior probability for each connection and averaging the values over 16 subjects. Second, the average values for all the thirty connections were tested against 0 by means of Statistical Packages for Social Sciences (SPSS) at significant level (α) = 0.05/[30 connections] (95% CI). Third, for any connection that is significant, it must be presented by at least 8 subjects with posterior probability larger than 0.9 so that it can be finally concluded that it is significant and the connectivity exist in at least half of the total number of subject under study. The most probable connectivity models for UNI_{left}, UNI_{right} and BIM are then suggested. Finally, the One-Way ANOVA was used on the most probable model for UNI_{left}, UNI_{right} and BIM to search for the existence of any significant difference at $\alpha = 0.05$ in the mean intrinsic connectivity among those connections that are significant by using the respective connections as factors and the connectivity values as the dependent list. Tukey post-hoc analysis for multiple comparison at $\alpha = 0.05$ will be used if there exist at least one pair of connections that shows significant difference in their connectivity values.

RESULTS

Demographical results

The average subjects' age and its standard deviation are 22.31 ± 2.65 years old. Five of the subjects were Chinese while the rest are Malays. All subjects were confirmed to be healthy and right-handed with the average laterality index of 76.25 (in the range of 4th right).

RFX analyses

Figure 2 shows the statistical parametric maps (SPMs) obtained from random-effects analysis (RFX) indicating contra-lateral and ipsi-lateral brain activations due to (a) UNI_{right}, (b) UNI_{left} and (c) BIM (BIM_{left} and BIM_{right}). The SPMs are overlaid onto Colin27T1_seg.img template. The crossing of the hair-lines indicates the point of maximum intensity which occurred at (-32,-22,50) and (38,-20,62) in the left and right hemispheres for UNI_{right} and UNI_{left} respectively. For BIM, the peak coordinates obtained from RFX are (-32,-22,50) in the left and (34,-20,50) in the right hemispheres. These coordinates have been confirmed to be located in the respective M1 regions in the left and right hemispheres and are comparable to the M1 coordinates obtained in a previous study[1]. In order for several ipsi-lateral regions to be visualised, the SPMs shown in Figure 2 are thresholded at $\alpha = 0.01$. Some significant clusters ($p < 0.001$) with their MNI coordinates at the point of maximum intensity due to UNI_{right}, UNI_{left} and BIM, as well as the respective anatomical areas in which the activation occurs are shown in Figure 3 (for BIM only) and summarised below.

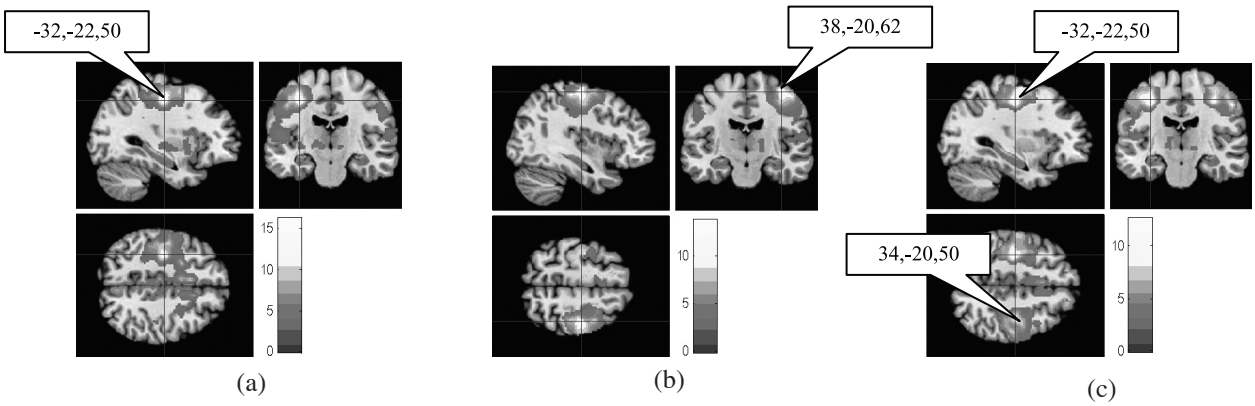

Figure 2: Statistical parametric maps (SPMs) obtained from random-effects (RFX) analysis (n = 16, $t > 2.60$, $p < 0.01$ uncorrected) showing brain activation due to (a) UNI_{right}, (b) UNI_{left} and (c) BIM overlaid onto structural brain images. Color codes represent increasing t value from red to white

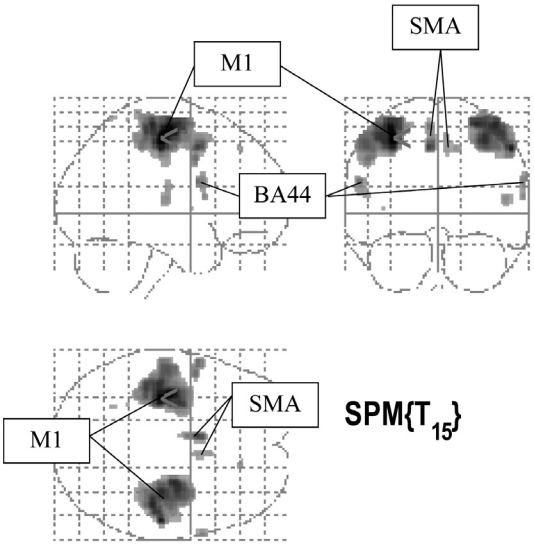

Figure 3: The SPMs obtained from RFX on all subjects for BIM at uncorrected α = 0.001 showing significant activation in the left and right M1, SMA and BA44

For UNI_{right}, 9 significant clusters survive a height threshold of uncorrected $\alpha = 0.001$ and a spatial threshold of 10 voxels. In this study, the clusters with the number of activated voxel of less than 10 are believed to be generated by factors not included in the experimental paradigm such as aliased biorhythm and mild responses of the brain during the experiment. There are a total of 4164 activated voxels ($t > 3.73$) in the main cluster which covers parts of the left post and precentral gyrii and left SMA. The eight highest peaks are at Talairach-MNI coordinates of (-32,-22,50), (-42,-18,52), (-42,-24,52), (-26,-16,64), (-36,-12,64), (-42,-36,46), (-46,-16,48) and (-6,6,48). The results indicate that 29.8% of the main cluster is in the left BA6 (27.8% activated), 9.7% of cluster is in the left BA2 (44.6% activated), 7.8% of cluster is in the left BA3b (50.9% activated) and 7.1% of cluster is in the left BA4p (52.5% activated).

For UNI_{left}, 4 significant clusters survive the uncorrected height threshold of $\alpha = 0.001$ and a spatial threshold of 10 voxels. The main activation cluster in the precentral gyrus consists of 5 maxima. Their Talairach-MNI coordinates are (38,-20,62), (42,-24,62), (36,-32,60), (46,-16,58) and (48,-22,58). A number of 2012 voxels are activated ($t > 3.73$); 35.0% of cluster is in the right BA6 (16.0% activated), 13.5% of cluster is in the right BA1 (32.7% activated), 10.2% of cluster is in the BA3b (22.5% activated) and 8.7% of cluster is in the right BA4a (15.2% activated).

For BIM, 9 major clusters of activation are revealed under a significant level of uncorrected $\alpha = 0.001$ ($t > 3.73$) and a spatial threshold of 10 voxels, occurring in the left and right precentral and postcentral gyrii, left and right SMA, right superior frontal gyrus, right Heschl's gyrus and right rolandic operculum. The primary cluster which is believed to be due to the control on right hand fingers has 5 maxima covering the left post and precentral gyrii which are centered at Talairach-MNI coordinates of (-32,-22,52), (-36,-16,60), (-30,-8,62), (-30,-12,64) and (-40,-32,60) respectively. This cluster has 2200 activated voxels ($t > 3.73$) from which 29.9% of the main cluster is in the left BA6 (14.9% activated), 14.5% is in the left BA1 (34.6% activated), 10.5% of cluster is in the left BA2 (25.8% activated) and 9.9% of cluster is in the left BA4p (39.1% activated). On the other side of hemisphere, the secondary cluster that resulted from left hand fingers coordination, has also 5 maxima, all located in the right pre and postcentral gyrii and right superior frontal gyrus. The maxima are centered at Talairach-MNI coordinates of (54,-22,46), (42,-28,62), (28,-12,64), (34,-22,52) and (46,-26,56). A number of 2142 voxels are activated in the main cluster ($t > 3.73$) from which 35.7% of this cluster is in the right BA6 (17.4% activated), 14.0% in the right BA1 (36.1% activated), 9.2% of cluster in the right BA3b (21.6% activated) and 8.5% in the right BA4a (15.9% activated).

BIM has also resulted in the activation of the left and right SMA which correspond to the third and fourth major clusters. For the left SMA, 81.5% of cluster is in the left BA6 (3.0%) activated. It has 2 maxima at Talairach-MNI coordinates of (-6,6,48) and (-6,-2,62). A number of 175 voxels are activated in this cluster ($t > 3.73$). For the right SMA, 83.8% of cluster is in the right BA6 (1.1% activated). The cluster also has 2 maxima at Talairach-MNI coordinates of (8,8,50) and (8,14,54) with a number of 60 activated voxel ($t > 3.73$).

Another interesting activation during BIM are indicated by symmetrical characteristic of clusters 7 and 9. Cluster 7 consists of 38 activated voxels ($t > 3.73$) which occur in the right precentral gyrus (64,8,22) and right Rolandic

operculum (64,10,12). It was found that 39.5% of cluster is in the right BA44 (1.7% activated) and 8.9% of cluster is in the right BA6. Whereas for cluster 9 (27 activated voxel; t > 3.73), 98.1% of cluster is in the left BA44 and 1.9% of cluster is in the left BA6. This cluster occurs in the left precentral gyrus (-56,6,22).

Conjunction analysis

The results obtained from the analysis of conjunction ($\alpha = 0.1$) on the present UNI_{right} and UNI_{left} datasets indicate that all subjects show common activation areas in the primary motor area. For UNI_{right}, 3 activation clusters are detected in the left postcentral gyrus and precentral gyrus. The main cluster which has 64 activated voxels ($t > 1.28$) with the point of maximum activation at (-34, -22, 54), shows that 55.1% of cluster is in the left BA4p (6.3% activated), 25.6% of cluster in the left BA4a (1.3% activated), 10.7% of cluster in the left BA6 (0.2% activated) and 8.6% of cluster is in the left BA3b (0.9% activated).

For UNI_{left}, the analysis of conjunction at significant level of $\alpha = 0.1$, reveals 1 cluster of activation which is in the right precentral gyrus. The cluster consists of 95 activated voxels ($t > 1.28$) and has 5 maxima with the highest two at (36, -20, 62) and (40, -14, 56). 89.9% of the cluster is in the right BA6 (1.9% activated), 8.2% is in the right BA4a (0.7% activated), 0.5% of cluster is in the right BA4p (0.1% activated) and 0.3% of cluster is in the right BA3b (0.1% activated).

The results for conjunction analysis on BIM reveal 3 significant clusters at $\alpha = 0.1$ which are located in the left and right precentral gyrus. For cluster 1, there are 18 activated voxels with 97.9% of cluster is in the left BA6. For cluster 2, 12 voxels are activated and 82.3% of cluster is in the right BA6. For cluster 3, only 2 voxels are activated and 100% of the cluster is in the right BA6.

Percentage of signal change

The percentage of change in signal intensity (PSC) that had occurred in the left and right M1, SMA and BA44 are tabulated in Table 2 for UNI_{right}, UNI_{left} and BIM. For UNI_{right}, M1-L, SMA-L and BA44-L show higher PSC values as compared to the ipsi-lateral M1-R, SMA-R and BA44-R. The PSC values for UNI_{left} are higher in M1-R and SMA-R as compared to the ipsi-lateral M1-L and M1-R, but the ipsi-lateral and contra-lateral values for BA44 are about the same. For BIM, SMA-L and BA44-L have higher PSC values as compared to SMA-R and BA44-R. However, the PSC for M1-R is slightly higher than the opposite M1-L. As opposed to number of activated voxels, the tapping of the left hand fingers generated higher signal change in M1-L than in M1-R during the tapping of right hand fingers. The effect is however incomparable in SMA and BA44.

Table 2: Percentage of signal change (PSC) in a spherical region about the peak coordinates of the right and left M1, SMA and PMC for UNI_{right}, UNI_{left} and BIM

	Percentage of signal change/%					
	M1-L	M1-R	SMA-L	SMA-R	BA44-L	BA44-R
UNI_{right}	1.650	0.633	0.860	0.670	0.688	0.643
UNI_{Left}	0.713	2.377	0.739	0.793	0.551	0.525
BIM	1.746	1.774	0.629	0.599	0.514	0.471

Dynamic causal models

Group Bayesian model selection (BMS) results for the left, right and bimanual finger tapping over 16 right handed subjects are shown in Figure 4(a), (b) and (c) respectively. The results are obtained by means of fixed (FFX) and random (RFX) effects analysis for BMS. The BMS results clearly show evidence of superiority of Model 7 for UNI_{left} and Model 6 for UNI_{right} as compared to the other 9 models indicating the right M1 as the most probable input center during left hand finger tapping and the left M1 for right hand finger tapping. For BIM, three models show a relatively high probability as compared to the other seven models but are unequally preferred as can be seen in Figure 4(c). The models are Models 2, 6 and 7. From RFX perspective, the winning model among the three models is obviously Model 6. However, since BIM is assumed to be coordinated by the primary motor area in both hemispheres, Model 2 is the most preferable model for BIM. Furthermore, Model 2 is seen to be the most probable model in FFX perspective with a high posterior model probability and relative log evidence. Table 3(a – c) summarises the group (RFX and FFX) BMS analyses for UNI_{left}, UNI_{right} and BIM respectively. All tapping types exhibit constant sum of negative free energy (F) for all models. The Dirichlet parameter estimates (α_d), expected posterior probability (<*r*>) and exceedance probability

(φ) obtained from RFX for BMS and log-evidence and posterior model probability (P) obtained from FFX for BMS show high preference for Model 7 as the most probable model for UNI_{left} and Model 6 for UNI_{right}. These two models will be further analysed in determining the effective connectivity between the ROIs for UNI_{left} and UNI_{right}. As for BIM, Model 2 is the model of choice for further analyses. The decision made in choosing these three models to represent UNI_{left}, UNI_{right} and BIM rests on the results obtained from both the FFX and RFX analyses for BMS as depicted in Table 3 and Figure 4. These models show consistent evidence of optimal models either in FFX or RFX analytical framework.

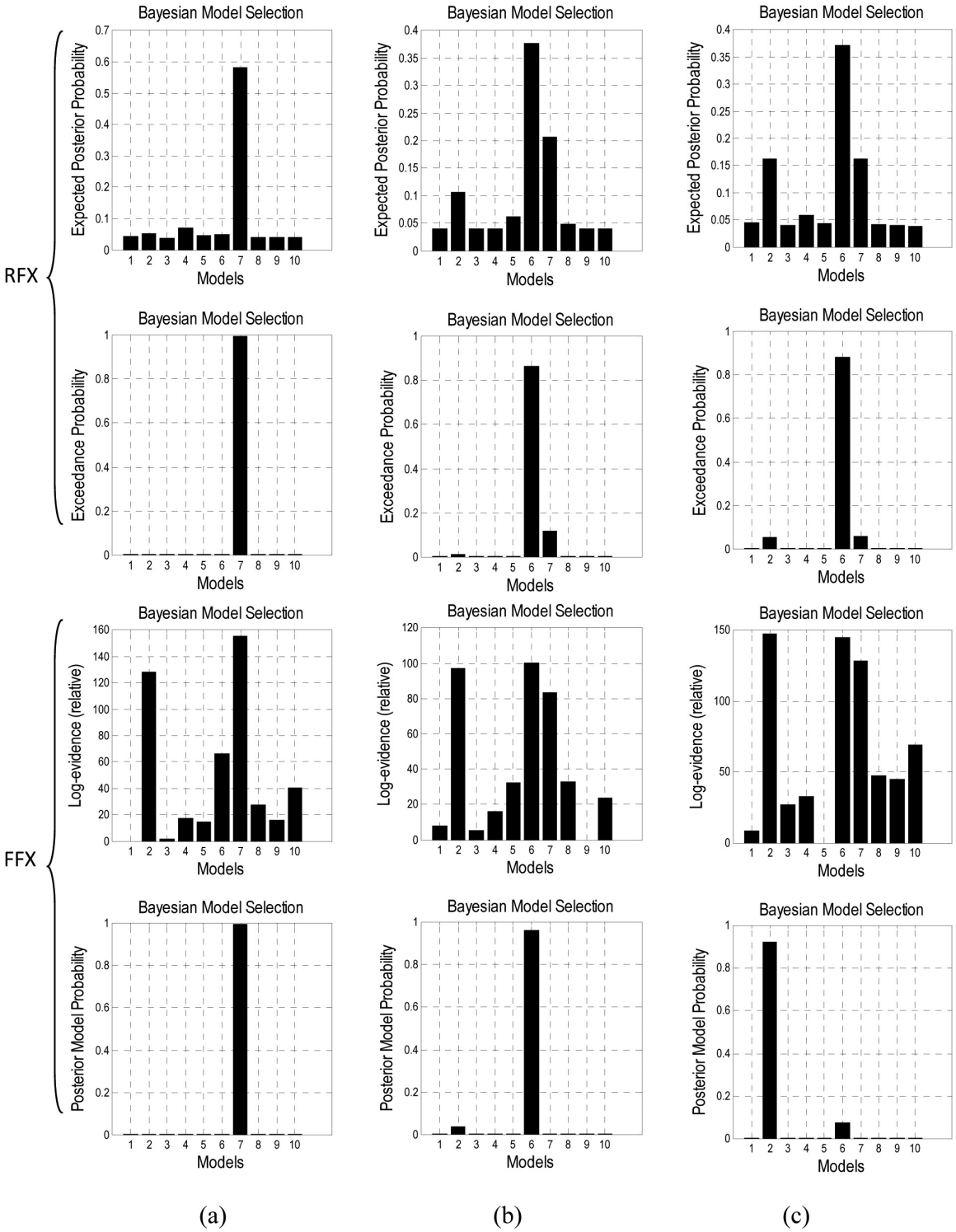

Figure 4: BMS histograms for a) UNI_{left}, b) UNI_{right} and c) BIM obtained from RFX (top) and FFX (bottom) showing preferences on models 7, 6 and 2 respectively

Table 3: BMS RFX and FFX results for a) UNI_{left}, b) UNI_{right} and c) BIM for the ten models obtained across the 16 subjects under study

(a)

	Model 1	Model 2	Model 3	Model 4	Model 5	Model 6	Model 7	Model 8	Model 9	Model 10
$-\Sigma F$ (x 10^4)	3.0542	3.0413	3.0540	3.0524	3.0527	3.0475	3.0386	3.0514	3.0526	3.0502
α_d	1.0945	1.3519	1.0027	1.7885	1.2282	1.3057	15.1320	1.0272	1.0462	1.0231
$<r>$	0.0421	0.0520	0.0386	0.0688	0.0472	0.0502	0.5820	0.0395	0.0402	0.0394
φ	0	0.0001	0	0.0002	0.0001	0.0001	0.9995	0	0	0
Log-evidence	0	128.00	1.65	17.50	14.40	66.60	156.00	27.90	15.80	40.30
P	1.27E-14	1.20E-12	1.27E-14	1.27E-14	1.27E-14	1.27E-14	1.0000	1.27E-14	1.27E-14	1.27E-14

(b)

	Model 1	Model 2	Model 3	Model 4	Model 5	Model 6	Model 7	Model 8	Model 9	Model 10
$-\Sigma F$ (x 10^4)	3.0360	3.0271	3.0363	3.0352	3.0336	3.0268	3.0285	3.0336	3.0368	3.0345
α_d	1.0287	2.7788	1.0390	1.0196	1.5950	9.8164	5.3925	1.2614	1.0304	1.0382
$<r>$	0.0396	0.1069	0.0400	0.0392	0.0613	0.3776	0.2074	0.0485	0.0396	0.0399
φ	0.0006	0.0118	0.0007	0.0006	0.0021	0.8659	0.1159	0.0011	0.0006	0.0007
Log-evidence	8.14	97.10	5.36	16.30	32.50	100.00	83.50	32.80	0	23.50
P	1.22E-14	0.0363	1.22E-14	1.22E-14	1.22E-14	0.964	4.19E-8	1.22E-14	1.22E-14	1.22E-14

(c)

	Model 1	Model 2	Model 3	Model 4	Model 5	Model 6	Model 7	Model 8	Model 9	Model 10
$-\Sigma F$ (x 10^4)	3.0253	3.0114	3.0235	3.0229	3.0262	3.0117	3.0133	3.0214	3.0217	3.0192
α_d	1.1527	4.2075	1.0212	1.5117	1.1185	9.6556	4.2332	1.0628	1.0224	1.0143
$<r>$	0.0443	0.1618	0.0393	0.0581	0.0430	0.3714	0.1628	0.0409	0.0393	0.0390
φ	0.0010	0.0549	0.0007	0.0021	0.0009	0.8821	0.0561	0.0008	0.0008	0.0007
Log evidence	8.42	147.00	26.90	32.80	0	145.00	128.00	47.40	44.80	69.20
P	1.17E-14	0.9234	1.17E-14	1.17E-14	1.17E-14	0.0766	5.25E-9	1.17E-14	1.17E-14	1.17E-14

Intrinsic connectivity

A detailed analysis conducted on Model 7 for UNI_{left} reveals intrinsic connectivity values resembled by the elements of the A matrix shown in Equation (1). The A matrix is a 6 × 6 matrix in which each matrix element represents the fixed or context-independent strength of connections between the modeled regions (intrinsic couplings). As can be seen in Figure 1, there are 30 possible connections with 30 intrinsic connectivity values for each model. For Model 7, the intrinsic input has been determined to be through the right M1. To test for the significance of the intrinsic input and connectivity values, the average values of the input and intrinsic connectivity for all connections for each subject is entered into a one-sample t-test with '0' as target value. All the inputs (M1-R) and majority of the connections are

found to be significant ($p < \alpha = 0.05/30$ connections $= 1.7 \times 10^{-3} \approx 0.002$; 95%CI). Insignificant ($p > 0.002$) connections are M1-L→M1-R, BA44-L→SMA-R, BA44-R→M1-R, BA44-R→SMA-R, SMA-R→M1-R, SMA-R→BA44-L and SMA-R→BA44-R. However, not all connections that are significant show posterior probability value higher than 0.9 which is the cut-off value for a connectivity between any two regions to be considered as significant in a Bayesian framework. The connectivities are small whenever their posterior probability is less than 0.9. In this study, for any high probability and significant connections to be accepted, it must be seen to occur in at least eight subjects. Connections that are significant and with a high occurence probability for UNI_{left} are M1-R→M1-L, M1-R→ BA44-L, M1-R→ BA44-R, M1-R→SMA-L, M1-R→SMA-R, which are evident in the majority of the subjects.

It can be concluded that during UNI_{left}, connectivity in the brain is represented by the unidirectional M1-R→M1-L, M1-R→BA44-L, M1-R→ BA44-R, M1-R→SMA-L, M1-R→SMA-R connections. The average intrinsic input (through M1) and intrinsic connectivity for connections obtained from Model 7 for UNI_{left} for all subjects together with their statistics are tabulated in Table 4(a).

Similar analyses were conducted on Model 6 for UNI_{right}. All the inputs (M1-L) and majority of the connections are again found to be significant ($p < \alpha = 0.05/30$ connections $= 1.7 \times 10^{-3} \approx 0.002$; 95%CI). There is no connection that is not significant ($p > 0.002$). For UNI_{right}, connections that are significant and with a high occurence probability are M1-L→M1-R, M1-L→BA44-L, M1-L→BA44-R, M1-L→SMA-L, M1-L→SMA-R, which are evident in the majority of the subjects. It can be concluded that during UNI_{right}, connectivity in the brain is represented by the unidirectional M1-L→M1-R, M1-L→BA44-L, M1-L→BA44-R, M1-L→SMA-L, M1-L→SMA-R connections. The average intrinsic input (through M1) and intrinsic connectivity for connections obtained from Model 6 for UNI_{right} for all subjects together with their statistics are tabulated in Table 4(b).

Table 4: The intrinsic input and connectivity values and their statistics for a) UNI_{left}, b) UNI_{right} and c) BIM obtained from high probability significance connections that had occurs in the majority of the subjects

(a)

	Input	Intrinsic connectivity				
	M1-R	M1-R to M1-L	M1-R to BA44-L	M1-R to BA44-R	M1-R to SMA-L	M1-R to SMA-R
Ave	0.2034	0.1759	0.1483	0.1224	0.1653	0.1300
SD	-0.1098	-0.0937	-0.0995	-0.0902	-0.0837	-0.1002
p	2.19E-06	1.87E-06	2.62E-05	7.02E-05	1.01E-06	1.09E-04
t	7.409	7.505	5.959	5.426	7.899	5.192
Occurence	15 subjects	11 subjects	11 subjects	11 Subjects	12 subjects	11 subjects

Ave = average, SD = standard deviation

(b)

	Input	Intrinsic connectivity				
	M1-L	M1-L to M1-R	M1-L to BA44-L	M1-L to BA44-R	M1-L to SMA-L	M1-L to SMA-R
Ave	0.1711	0.2427	0.1624	0.1823	0.196	0.1544
SD	0.0517	0.096	0.0585	0.0806	0.0672	0.0826
p	1.10E-09	4.29E-08	1.25E-08	1.83E-07	6.39E-09	1.96E-06
t	13.253	10.117	11.098	9.051	11.661	7.476
Occurence	16 subjects	13 subjects	14 subjects	13 subjects	14 subjects	11 subjects

Ave = average, SD = standard deviation

(c)

	Input		Intrinsic connectivity				
	M1-L	M1-R	M1-L to BA44-L	M1-L to SMA-L	M1-L to SMA-R	M1-R to SMA-L	M1-R to SMA-R
Ave	0.1252	0.1733	0.119	0.1362	0.1304	1.281	0.1271
SD	0.0373	0.0269	0.0572	0.0482	0.0772	0.0487	0.0815
p	9.13E-10	8.01E-03	5.25E-07	9.88E-09	5.17E-05	2.59E-08	1.58E-05
t	13.432	3.055	8.325	11.292	6.76	10.51	6.241
Occurence	16 subjects	16 subjects	8 subjects	10 subjects	8 subjects	9 subjects	9 subjects

Ave = average, SD = standard deviation

For BIM, the above mentioned analyses were implemented on Model 2. The input M1-L was found to be significant ($p < 0.002$) while M1-R was not ($p > 0.002$). Both inputs however indicate high occurrence probability in all subjects. All intrinsic connections were found to be significant ($p < 0.002$) except for the SMA-R→SMA-L connection which has a p value of 0.008. For BIM, connections that are significant and with a high occurence probability are M1-L→BA44-L, M1-L→SMA-L, M1-L→SMA-R, M1-R→SMA-L, M1-R→SMA-R, which are evident in at least half of the number of subjects. It can be concluded that during BIM, connectivity in the brain is represented by the unidirectional M1-L→BA44-L, M1-L→SMA-L, M1-L→SMA-R, M1-R→SMA-L, M1-R→SMA-R connections. The average intrinsic input (through M1-L and M1-R) and intrinsic connectivity for connections obtained from Model 2 for BIM for all subjects together with their statistics are tabulated in Table 4(c). Figure 5 summarises the intrinsic connectivity model for UNI_{left}, UNI_{right} and BIM.

The results obtained from One-Way ANOVA indicate no significant difference among the significant connections for UNI_{left} ($F = 0.938$, $p = 0.447$) and BIM ($F = 0.894$, $p = 0.489$). However, for UNI_{right}, significant difference was found to exist ($F = 3.204$, $p = 0.017$) between M1-L→M1-R and M1-L→BA44-L ($p = 0.037$) as well as between M1-L→M1-R and M1-L→SMA-R ($p = 0.037$) connections after performing Tukey post-hoc test for multiple comparison.

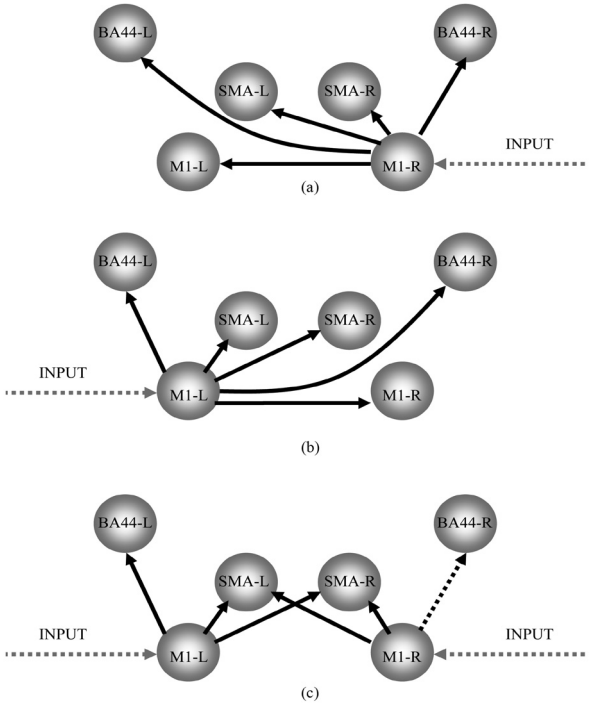

Figure 5: Intrinsic connectivity models for a) UNI_{left}, b) UNI_{right} and c) BIM

DISCUSSION

Individual subject activation

The activation patterns obtained from individual subject are not perfectly the same in terms of activation area and intensity despite the fact that all subjects performed similar task. For example, not all subjects activate a particular brain region and any one subject may experience activation in many different areas than others and with different activation magnitudes. The differences between the results obtained from individual analysis on all subjects clearly show the subject-specific effects which are not always the same from subject-to-subject due to the intrinsic variability in each particular subject. These could be due to the differences in the blood oxygenation level dependent (BOLD) signal intensity that is captured from each subject and may also arise due to subjects' different brain sensitivity when the task is performed, since the vasodilatory signal, cerebral blood flow (CBF), cerebral blood volume (CBV) and the quantity of deoxyhemoglobin which govern the height and spatial extent of the activation in the brain, differ significantly in all individuals. The variability is thought to be intrinsic in nature since precautions in reducing the effects from confounding factors have been taken into consideration so as to ensure that the fMRI experiment performed on all subjects is as similar as possible. Another possible source of variability is the inconsistency of the force and pace used by the subjects to tap their fingers, despite the training and tutorial given to the subjects prior to the fMRI scans. Previous studies[26 & 27] indicate that brain activation in cerebral motor cortices does depend on tapping frequency as well as tapping force. However, since the objective of this study was mainly focused on self-paced type of movement, large differences in tapping force and frequency between subjects are expected to occur among subjects, hence robustness, and will be taken into consideration in the interpretation of results. The fact that subjects' movements are not contributing to the observed activation is acceptable since those movement related effects, in particular the translational (*x, y* and *z*) as well as rotational (pitch, roll and yaw) motions have been excluded in generating the contrast images.

RFX and conjunction results

From Figure 2 and the summarisation of the SPMs results given previously, it is quite interesting to see that the left side of the brain (triggered by the tapping of the right hand fingers) shows a larger number of activated voxels as compared to the right side of the brain (triggered by the left-hand finger tapping). For BIM, the number of activated voxel in the left hemisphere is only slightly higher than in the right hemisphere and the activated voxels in the left hemisphere is much less as compared to that in the left hemisphere due to UNI_{left}. These results are in contrast to that obtained from our previous study on a single right-handed male subject[12], despite the fact that all the subjects are right handed, but are in consistent with the other study[13] conducted on seven right-handed female subjects. This explains how reliable a multiple subject analysis is, in making inference over a population. Moreover, group results indicate the existence of ipsi-laterality accompanying the expected contra-laterality.

The analyses conducted were focused on three bilateral anatomical regions from which two are known to be involved in controlling motor movement; the primary motor cortex in the precentral gyrus (named as M1) and SMA which is also known to be involved in planning complex movements and in coordinating movements involving both hands[3]. The other area is BA44. The reasons behind the inclusion of BA44 are 1) it is symmetrically activated at α = 0.001 especially for BIM, 2) due to one of its functions which is speech and language processing and 3) to enable study on the connectivity between motor regions and other regions not related to motor coordination but have significant activation. Speech and language areas should have reveal certain extent of activation in this study since the interchange between UNI_{left}, UNI_{right} and BIM tapping is done via verbal instruction using the intercom i.e. "START LEFT", "STOP LEFT" or "START RIGHT", "STOP RIGHT".

The M1, SMA and BA44 were found to be activated at different significant level in all of the participating subjects but the coordinates of the activation peak differ by a few millimeters from subject to subject. Differences in activation can also be observed when comparing between the left and right hemisphere regions. Group RFX results for BIM shown in Figure 3 clearly indicate a larger spatial extent of activation in the left SMA and BA44 as compared to the right, while the spatial extent of activation for M1 is quite symmetrical. The larger spatial extent of activation for left BA44 as compared to the right can be easily understood since the processing of speech and language are more likely to occur in the left hemisphere. However, a similar effect that occur on SMA is not known and needs further clarification.

The typicality of the effects of the unilateral and bilateral tapping of hand fingers in all subjects was investigated using conjunction analysis. Conjunction analysis[21] provides a way to locate common features of functional anatomy between subjects under the same experimental condition. The results obtained from the analyses of conjunction on the present UNI_{right}, UNI_{left} and BIM datasets indicate that all subjects show common activation areas in precentral gyrus (M1). Due to the relatively high variability among the subjects under study, the SPM results generated at significant level of α = 0.1 indicate significant activation only at voxel level. Both the set and cluster level inferences about the activation clusters revealed insignificant brain activation. Conjunction analyses results therefore confirm the central

role of M1 in coordinating the three finger tapping tasks used in this study.

In our previous study on a single right-handed male subject[12], we found that the activated primary motor areas in the right hemisphere due to UNI_{left} showed a higher signal intensity and larger activation area as compared to that in the left hemisphere due to UNI_{right}. We also found that the right hemisphere exhibited larger activation area during BIM. The findings obtained from our single subject study are in good agreement with a multiple subject fMRI study on unilateral and bilateral sequential movement in right-handers[26]. They found that the right hemisphere showed more activation than the left hemisphere in both unilateral and bilateral task at two tapping frequencies. They also concluded that faster movement rates will cause higher activation both in terms of signal intensity and number of activated voxel, the so called "rate effects". Their interpretations are that right-handers expend more effort to perform with their non-preferred hand. A stronger activation pattern in the right hemisphere is the result of trying to perform with a system that is slightly less competent with the implication that the more skilled and competent system will expend less effort and will therefore provide a weaker activation. As for the rate effects, they concluded that faster movement involves the recruitment of more motor units and will therefore activate a greater number of voxels. Their findings had later be reconfirmed[10].

However, in this study and in our separate study on seven right-handed female subjects[13], we found that the average responses obtained from FFX (not shown) and RFX indicate higher height (signal intensity) and spatial (activation area) extent of activation in the left hemisphere for unilateral type of finger tapping. As mentioned earlier, this study used a robust self-paced finger tapping. Prior to the fMRI scan, the subjects were told that they need to tap their fingers two times in one second using an intermediate force between too soft and too hard. However, since all the subjects are right-hand dominant, there would be a tendency for the subjects to tap their preferred hand fingers faster than their non-preferred hand fingers, resulting in the rate effects. Based on the interpretation given above, it seemed that the influence of the rate effects is greater than the effects that would be produced by the average effects of the dominant and sub-dominant hand, hence greater spatial activation in the left hemisphere. A larger activation area could also be due to the tendency of these right-handers to press their fingers harder against the thumb using their dominant hand fingers, whereby a larger force will activate a larger area with higher intensity. Interestingly, in contrast to the spatial extent of activation, the height extent or PSC for M1 obtained in this study is higher in the right hemisphere (due to UNI_{left}) as compared to the PSC measured in the left hemisphere (due to UNI_{right}), see Table 2. This finding is in contrast to the number of activated voxels which is higher for UNI_{right} as compared to UNI_{left}. PSC is defined as the relative signal change within a cytoarchitectonic area evoked by the different experimental conditions, which reflects the involvement of that particular area in a specific task[23]. It is simply the ratio between the condition-specific signal change and the mean signal during the session. In relation to the discussion above, it can be assumed that tapping rate does not influence the height extent of activation as it does on the spatial extent of activation. As a result, the higher PSC observed in the right hemisphere is due only to a higher control demand used by the brain in coordinating the tapping of the sub-dominant hand fingers.

For BIM, the height and spatial extents of activation are almost similar between the left and right M1, SMA as well as BA44. Group results indicate relatively small differences in the number of activated voxel and percentage of signal change as can be seen in Table 2 and Figure 3. The findings are consistent with a previous study[1] which indicate symmetrical spatial extent of activation in M1 and SMA. The effects observed for bimanual however are different from the resultant effects of combining between UNI_{left} and UNI_{right}. Thus, for a bimanual type of finger tapping, it can be concluded that the effects obtained are not the sum of the effects produced individually by UNI_{left} and UNI_{right} as reported[3].

The results depicted in Figure 2, and Table 2 clearly revealed significant activated areas in the opposite hemisphere to the contra-lateral hemisphere. For UNI_{right}, ipsi-lateral activation occurs in the right postcentral gyrus, right Rolandic operculum, right precentral gyrus, right middle frontal gyrus, right superior frontal gyrus, right SMA and right middle cingulate gyrus. For UNI_{left}, the ipsi-lateral areas are left precentral gyrus, left SMA and left middle frontal gyrus. The existence of ipsi-lateral activation in motor cortex has been widely reported and discussed[1, 3, 28]. It shows evidence of involvement of ipsi-lateral areas in coordinating motor movement. One of the observed effects related to ipsi-lateral activation is inhibition whereby increased neuronal activation in motor area of one hemisphere suppresses neuronal activity of the same area in the opposite hemisphere. Inhibitory has been shown to be either in terms of activated volume or percentage of signal change[28]. In terms of functional specialisation, inhibition is not observable in this study since tapping style is kept constant. However, as can be seen from Figure 2 and Table 2, ipsi-laterality did occur in both M1 and SMA and the effects are asymetrical and these show possible evidence of inhibitory of activation in the ipsi-lateral areas.

Effective connectivity

It has been established that the primary motor area (M1) in the precentral gyrus (PCG) and the supplementary motor

area (SMA) in the medial dorsal wall are involved in movement preparation and execution of motor action. While M1 and SMA are known to be responsible in triggering and initiating motor related movements, SMA has a special function of being able to coordinates interlimbs movements spatially and temporaly especially during bilateral execution[11]. It is evident from Figure 2 that both areas are also involved even in unilateral types of movement suggesting the existence of interhemispheric connectivity between these areas. The inclusion of the left and right BA44 in this study was motivated by their significant activation on uncorrected (α = 0.001) SPMs. It is hypothesized that the left and right BA44 were also connected to the motor areas during the execution of self-paced motor task since the tapping instructions were given verbally via headphones i.e involving speech and language.

In the present study, we investigated the intrinsic couplings only between M1, BA44 and SMA of the right and left hemispheres. The pre-motor cortex (PMC), another important area in motor coordination is not included in the present study due to the inconsistency of the activation in the respective area for all subjects, even at a lower significance level, resulting in lack of activation in group results. This could be due to the nature of task done by the subjects that does not involve the integration of sensory information which is one of the functions of PMC.

Biophysically plausible time-series models that reasonably represent interacting cortical regions can be constructed based on Equation (1). The models may consist of all of the three intrinsic couplings, modulatory and extrinsic inputs or may consist of only the intrinsic couplings and extrinsic inputs, depending on the experimental design[5]. In this study, we use only the extrinsic inputs and intrinsic couplings. Due to experimental limitations, contextual or modulatory input was not included to be estimated by DCM in the present study since no such stimulus was given to the subject so that there is at least one area in the brain that will be influenced by contextual input.

Based on Equation (1) and the activation obtained in Figure 2 and 3, we constructed ten biologically and physically plausible models that consisted of M1, BA44 and SMA in both hemispheres as shown in Figure 1. We hypothesised that the input will either be through M1, BA44 or SMA, unilaterally or bilaterally. To determine which region or regions that will most probably act as the input, our assumption was that any one region is fully connected to any other regions. Therefore, one may see that there are many other alternative models that can be constructed using the right and left M1 and SMA as processing centers, with a large number of mathematically possible connections. However, we limited this study to the ten biologically physically plausible models that we believed would be able to explain the intrinsic couplings between M1, BA44 and SMA in both hemispheres during UNI_{left}, UNI_{right} and BIM.

DCM uses a fully Bayesian approach in estimating and selecting the most probable model among the competing models. According to Bayes' rule, the posterior distribution is equal to the likelihood times the prior devided by the evidence[9] or $p(\theta|y\ ,m) = [p(y|\theta\ ,m)\ p(\theta|m)]/p(y|m)$. Taking logs for both sides; $\log p(\theta|y\ ,m) = \log p(y|\theta\ ,m) + \log p(\theta|m) - \log p(y|m)$. The expression $p(y|m)$ is the probability of obtaining observed data y given a particular model m, also named as model evidence while $p(\theta|m)$ is the probability of obtaining DCM parameters θ given a particular model m which is named as prior. The expression $p(y|\theta\ ,m)$ is the probability of obtaining observed data y given DCM parameters θ and a particular model m also named as likelihood and $p(\theta|y\ ,m)$ is the probability of obtaining DCM parameters θ given data y and a particular model m also named as posterior distribution.

The results obtained from Bayesian model selection (BMS) for group RFX and FFX studies are shown in Table 3 and Figure 4 for comparison. The constant values of the sum of negative free energy (ΣF) for UNI_{right}, UNI_{left} and BIM indicate a perfect balance between accuracy and complexity[19] for all models shown in Figure 1. The fact that the values are almost the same for all types of movement also reflects a good fitting of the models to the observed data regardless of the types of movement. The related equation is $F = \langle \log p(y|\theta\ ,m) \rangle_q - \mathrm{KL}[q(\theta), p(\theta|m)]$[19]. Accuracy or the log likelihood is the first term on the right side of the equation which explains the probability of obtaining observed data y given DCM parameters θ and a particular model m. Complexity is reflected in the second term which contains the amount of information that can be obtained from the data with regards to the parameters of a model.

The Dirichlet parameter estimates (α_d), the expected posterior probability ($<r>$) and the exceedance probability (φ) are all the parameters used in BMS analyses to rank models at group RFX level. The Dirichlet parameter estimates is a measure of effective number of subjects in which a given model generated the observed data. The sum of all α_d is equal to the number of subjects plus the number of compared models. The exceedance probability φ_k is the probability that a given model k is more likely than any other model to give the observed experimental data. If φ_k obtained for model k from K models is 0.95 (or 95%), one can be 95% sure that the favoured model has a greater posterior probability $<r>$ than any other tested models. As can be seen in Table 3, the sum of φ is unity. The histograms in Figure 4 (top) graphically indicate the expected posterior probability and the exceedance probability for all models. Both two quantities for Model 7 and Model 6 for UNI_{left}, UNI_{right} are comparatively higher than any other models. From Table 3, it can be seen that all the values of α_d, φ and $<r>$ agree very well that both the UNI_{left} and UNI_{right} are best represented by Model 7 and Model 6 respectively. Furthermore, these two models have also shown firm evidence in FFX perspective with a high posterior model probability (P) in getting the respective log evidences, see Table 3 and Figure 4 (bottom). However, for BIM, even though the RFX for BMS results indicate Model 6 as the most probable

model, it is not the preferred model in FFX perspective. FFX for BMS instead, has choosen Model 2 as the most probable model for BIM with the log-evidence of 147 and posterior model probability of 0.9234 as opposed to 145 and 0.0766 for Model 6. In view of the model structure used in this study that is assumed to be identical across subjects[29], the results obtained from FFX for BMS are more reliable. Therefore, Model 2 is the model of choice for BIM. More importantly, the results obtained from group BMS studies whether in RFX or FFX perspectives, have been reported[29] to be able to take into consideration the presence of outliers that could have arisen in any subject under study. Thus BMS analysis is the preferred approach in model comparison involving multiple subjects.

Model 7 and Model 6 which have been proven to be the winning models among the ten competing models for UNI_{left} and UNI_{right} have six ROIs that are fully connected to any other ROI. The values depicted in Table 4(a) and (b) represent the acceptable average extrinsic input and intrinsic couplings between the ROIs for Model 7 and Model 6. As mentioned previously, this study excluded contextual or modulatory input. Therefore, the acceptable intrinsic coupling values in Table 4(a) and (b) are basically the element of **A** matrix in Equation (1), while the values in the input column are the element of matrix **C**. Also shown in the tables are the statistics obtained from one-sample t-test to test whether the average values for the connections over the 16 subjects are significant or not against the condition of no connection, i.e. '0'. The effect size (t value) and p values indicate that all inputs and connections are significant. However, an effective connectivity between any two ROIs can be accepted if its value is relatively high with a posterior probability greater than 0.9[5]. For UNI_{right} and UNI_{left}, not a single connection has all subjects with posterior probability larger than 0.9. However, connections that have more than half of the number of subjects with posterior probability equal or larger than 0.9 are M1-L→M1-R, M1-L→BA44-L, M1-L→BA44-R, M1-L→SMA-L, M1-L→SMA-R for UNI_{right} and M1-R→M1-L, M1-R→BA44-L, M1-R→ BA44-R, M1-R→SMA-L, M1-R→SMA-R for UNI_{left}. Therefore, only these connections are considered for the construction of the most probable model for UNI_{right} and UNI_{left}. The models are schematically shown in Figure 5(a) and (b) for UNI_{left} and UNI_{right} respectively.

From this robust finger tapping study that involves 16 healthy young male and female right-handed adults, it can be summarised that during the unilateral tapping of left hand fingers, M1-R will act as the input centre, controlling the movement by triggering the synaptic signal unidirectionally to M1, BA44 and SMA contra- and ipsi-lateral to it. Similar transmission of signal is observed for UNI_{right} from which M1-L is found to be the input centre.

For BIM, significant connections found for M1-L→BA44-L, M1-L→SMA-L, M1-L→SMAR-R, M1-R→SMA-L and M1-R→SMA-R are evident in at least half of the number of subjects under study. This final intrinsic connectivity model (Figure 5 (c)) which is obtained from Model 2 is supposed to be symmetrical in nature. However, connectivity from M1-R to BA44-R (represented by dotted arrow) is found to be significant (posterior probability equal or larger than 0.9) in only four subjects. The input centers for BIM are the left and right M1. It is interesting to see from the results that M1-R-M1-L foward and backward connectivity is inhibited during BIM while it occurs unidirectionally during UNI_{left} and UNI_{right} from the contra-lateral to the ipsi-lateral regions. The inhibition of M1-M1 connection during BIM suggests that the primary motor area contra-lateral to the side of movement is not influenced by the one in the ipsi-lateral side in coordinating BIM type of movement. The synaptic signals triggered in any one M1 however, are sent to SMA in both sides of the brain during the coordination. It can also be observed that the left and right SMA and BA44 are not mutually connected during BIM and this can also be seen either during UNI_{left} or UNI_{right}.

From Figure 5, one can notice that no backward connection exist in all types of finger tapping conducted by this group of subjects. All connectivities originate from M1 contra-lateral to the side of movement for UNI_{left} and UNI_{right} and from both the left and right M1s for BIM. For unimanual type of finger tapping, the regions of M1 ispsi-lateral, left and right BA44 and left and right SMA receive information form M1 contra-lateral in maintaining the coordination of motor task. This includes information needed in maintaining the pace and force of tapping, maintaining the side of movement untill further instruction by understanding the previous instruction and maintaining the stability of tapping. For bimanual tapping of hand fingers, similar kind of coordination is thought to occur but with several inhibition of connectivity as compared to unimanual type of tapping, as mentioned previously. This again indicate that connectivity observed for BIM is not the sum of the connectivity for UNI_{left} and UNI_{right}.

For UNI_{left} and BIM, the difference in the strength of connection obtained from One-Way ANNOVA analyses between the connections that are significant is relatively small and not significantly different from one another. Whereas for UNI_{right}, significant difference is indicated in two out of ten comparisons. This behaviour of cortical network is analogous to the distribution of current at a junction in a parallel electrical circuit that has a comparable amount of load in each junction whereby the same amount of electrical charges flowing through each junction under the same potential difference. It is assumed that the input center, which is M1 served as the hub, producing and propagating the synaptic signal of the same magnitude to all other ROIs, from which the connectivity is said to occur under the same potential difference, hence the coordination of UNI_{left}, UNI_{right} and BIM.

CONCLUSION

The studies of functional specialisation and effective connectivity between activated regions in the brain evoked by

experimental manipulation i.e. unilateral tapping of hand fingers (UNI_{right} and UNI_{left}), has been made possible using noninvasive functional magnetic resonance imaging (fMRI) technique and a novel analyses of statistical parametric mapping (SPM), dynamic causal modeling (DCM) and Bayesian model selection (BMS) for group studies. The tapping rate effect was found to be greater than what would be produced by the average effects of the dominant and sub-dominant hand. The higher PSC observed in the right M1 however, is due to a higher control demand used by the brain in coordinating the tapping of the sub-dominant hand fingers. Ten biophysically plausible models constructed based on low-threshold activation of specific regions of interest (ROIs) were estimated and compared in a powerful Bayesian framework. The results of Bayesian model selection (BMS) for group studies that point to the most probable model for UNI_{left}, UNI_{right} and BIM with M1 as the input, indicating the reliability of the methods and reproducibility of the results. The primary motor area M1 in both hemispheres was determined to be the input centre during the unimanual and bimanual tapping of hand fingers. Significant connections between the ROIs are M1-L→M1-R, M1-L→BA44-L, M1-L→BA44-R, M1-L→SMA-L, M1-L→SMA-R for UNI_{right} and M1-R→M1-L, M1-R→BA44-L, M1-R→ BA44-R, M1-R→SMA-L, M1-R→SMA-R for UNIleft. For BIM, significant connection exist for M1-L→BA44-L, M1-L→ SMA-L, M1-L→SMAR-R, M1-R→SMA-L and M1-R→SMA-R. All significant connections are unidirectional in nature, i.e. no backward connection exist in UNI_{right}, UNI_{left} or BIM. The analyses implemented in this study reveal not only the specialisation of M1, BA44 and SMA during the coordination of unimanual and bimanual movement of hand fingers but also the couplings of interaction between the two regions within and between hemispheres. While M1-M1 connection has been found to be unidirectional for UNI_{right} and UNI_{left}, it is inhibited during BIM. The SMA-SMA and BA44-BA44 connections shows no evidence of significant connectivity for all conditions. On average, it can be said that for connections that are significant, there exist no significant difference between them.

ACKNOWLEDGEMENT

The authors would like to thank Sa'don Samian, the MRI Technologist of Universiti Kebangsaan Malaysia Hospital (HUKM), for the assistance in the scanning and the Department of Radiology, Universiti Kebangsaan Malaysia Hospital for the permission to use the MRI scanner. The authors were also indebted to Professor Karl J. Friston and the functional imaging group of the University College of London for valuable discussions on experimental methods and data analyses. This work is supported by the research grants IRPA 09-02-02-0119EA296 and eScience Fund 06-01-02-SF0548, the Ministry of Science, Technology and Innovation of Malaysia and UKM-GUP-SK-07-20-205, Universiti Kebangsaan Malaysia research grant.

REFERENCES

[1] Grefkes C, Eickhoff SB, Nowak DA, Dafotakis M, Fink GR. Dynamic intra- and interhemispheric interactions during unilateral and bilateral hand movements assessed with fMRI and DCM. Neuroimage 2008; 41: 1382–1394.

[2] Kasess CH, Windischberger C, Cunnington R, *et al.* The suppressive influence of SMA on M1 in motor imagery revealed by fMRI and dynamic causal modeling. Neuroimage 2008; 40: 828–837.

[3] Walsh RR, Small SL, Chen EE, Solodkin A. Network activation during bimanual movements in humans. Neuroimage 2008; 43: 540–553.

[4] Buchel C, Friston KJ. Modulation of connectivity in visual pathways by attention: cortical interactions evaluated with structural equation modeling and fMRI. Cerebral Cortex 1997; 7: 768 –778.

[5] Friston KJ, Harrison L, Penny W. Dynamic causal modeling. Neuroimage 2003; 19: 1273–1302.

[6] Kiebel SJ, Klöppel S, Weiskopf N, Friston KJ. Dynamic causal modeling: A generative model of slice timing in fMRI. Neuroimage 2007; 34: 1487–1496.

[7] Penny WD, Stephan KE, Mechelli A, Friston KJ. Modelling functional integration: a comparison of structural equation and dynamic causal models. Neuroimage 2004; 23: S264–S274.

[8] Toga AW, Thompson PM. An introduction to maps and atlases of the brain. In: Toga AW, Mazziotta JC, eds. Brain Mapping: The Systems. San Diego: Academic Press, 2000: 3–32.

[9] Penny WD, Stephan KE, Mechelli A, Friston KJ. Comparing dynamic causal model. Neuroimage 2004; 22: 1157–1172.

[10] Lutz K, Koeneke S, Wustenberg T, Jäncke L. Asymmetry of cortical activation during maximum and convenient tapping speed. Neuroscience Letters 2005; 373: 61–66.

[11] Aramaki Y, Honda M, Sadato N. Suppression of the non-dominant motor cortex during bimanual symmetric finger movement: A functional magnetic resonance imaging study. Neuroscience 2006; 141: 2147–2153.

[12] Yusoff AN, Hashim MH, Ayob MM, *et al*. Functional specialisation and connectivity in cerebral motor cortices: A single subject study using fMRI and Statistical Parametric Mapping. Malaysian Journal of Medicine and Health Sciences 2006; 2: 37–60.

[13] Yusoff AN, Mohamad M, Abd Hamid AI, *et al*. Functional specialisation and effective connectivity in cerebral motor cortices: An fMRI study on seven right handed female subjects. Malaysian Journal of Medicine and Health Sciences 2010; 6(2): 71 – 92.

[14] Yusoff AN, Mohamad M, Abdul Hamid K, *et al*. Activation characteristics of the primary motor area (M1) and supplementary motor area (SMA) during robust unilateral finger tapping task. Malaysian Journal of Health Sciences 2010; 8(2): (in press).

[15] Yusoff AN, Mohamad M, Abdul Hamid K *et al*. Intrinsic couplings between M1 and SMA during unilateral finger tapping task. Academy Science Malaysia Science Journal 2010; 4(2): (in press).

[16] Abe N, Suzuki M, Tsukiura T, *et al*. Dissociable roles of prefrontal and anterior cingulated cortices in deception. Cerebral Cortex 2006; 16: 192–199.

[17] NT Le DS, Pannacciulli N, Chen K, *et al*. Less activation of the left dorsolateral prefrontal cortex in response to a meal: a feature of obesity. American Journal of Clinical Nutrition 2006; 84: 725–731.

[18] Thiel CM, Fink GR. Visual and auditory alertness: Modality-specific and supramodal neural mechanisms and their modulation by nicotine. Journal of Neurophysiology 2007; 97: 2758–2768.

[19] Stephan KE, Penny WD, Daunizeau J, Moran RJ, Friston KJ. Bayesian model selection for group studies. Neuroimage 2009; 46: 1004–1017.

[20] Oldfield R. The assessment and analysis of handedness: the Edinburgh inventory. Neuropsychologia 1971; 9: 97–113.

[21] Friston KJ. Experimental design and statistical parametric mapping. In Frackowiak RSJ, Friston KJ, Frith CD, *et al*. eds. Human Brain Function. Amsterdam: Elsevier Academic Press, 2004: 599–632.

[22] Ashburner J, Friston KJ. Computational Neuroanatomy. In Frackowiak RSJ, Friston KJ, Frith CD, *et al*. eds. Human Brain Function. Amsterdam: Elsevier Academic Press, 2004: 655–672.

[23] Eickhoff SB, Stephan KE, Mohlberg H, *et al*. A new SPM toolbox for combining probabilistic cytoarchitectonic maps and functional imaging data. NeuroImage 2005; 25: 1325–1335.

[24] Brett M, Anton J-L, Valabregue R, Poline J-B. Region of interest analysis using an SPM toolbox. Proceedings of the 8th International Conference on Functional Mapping of the Human Brain; 2002 Jun 2 – 6: Sendai Japan. Available in CD-ROM in NeuroImage 2002 16(2).

[25] Stephan KE, Weiskopf N, Drysdale PM, Robinson PA, Friston KJ. Comparing hemodynamic models with DCM. Neuroimage 2007; 38: 387–401.

[26] Jäncke L, Peters M, Schlaug G, *et al*. Differential magnetic resonance signal change in human sensorimotor cortex to finger movements of different rate of the dominant and subdominant hand. Cognitive Brain Research 1998; 6, 279–284.

[27] Wildgruber D, Erb M, Klose U, *et al*. Sequential activation of supplementary motor area and primary motor

cortex during self-paced finger movement in human evaluated by functional MRI. Neuroscience Letters 1997; 227: 161–164.

[28] Newton JM, Sunderland A, Gowland PA. fMRI signal decrease in ipsilateral primary motor cortex during unilateral hand movements are related to duration and side of movement. NeuroImage 2005; 24: 1080 –1087.

[29] Stephan KE, Penny WD, Moran RJ, *et al*. Ten simple rules for dynamic causal modeling. Neuroimage 2010; 49: 3099–3109.